Hydrol. Earth Syst. Sci. Discuss., 11, 3857–3909, 2014
www.hydrol-earth-syst-sci-discuss.net/11/3857/2014/
doi:10.5194/hessd-11-3857-2014

Hydrology and Earth System Sciences
Open Access
Discussions

Large-scale regionalization of water table depth in peatlands optimized for greenhouse gas emission upscaling

M. Bechtold[1], **B. Tiemeyer**[1], **A. Laggner**[1], **T. Leppelt**[1], **E. Frahm**[1,*], **and S. Belting**[1,2]

[1]Thünen Institute of Climate-Smart Agriculture, Braunschweig, Germany
[2]Belting Umweltplanung, Quernheim, Germany
[*]now at: Physikalisch-Technische Bundesanstalt, Braunschweig, Germany

Received: 18 March 2014 – Accepted: 28 March 2014 – Published: 7 April 2014

Correspondence to: M. Bechtold (michel.bechtold@ti.bund.de)

Published by Copernicus Publications on behalf of the European Geosciences Union.

Abstract

Fluxes of the three main greenhouse gases (GHG) CO_2, CH_4 and N_2O from peat and other organic soils are strongly controlled by water table depth. Information about the spatial distribution of water level is thus a crucial input parameter when upscaling GHG emissions to large scales. Here, we investigate the potential of statistical modeling for the regionalization of water levels in organic soils when data covers only a small fraction of the peatlands of the final map. Our study area is Germany. Phreatic water level data from 53 peatlands in Germany were compiled in a new dataset comprising 1094 dip wells and 7155 years of data. For each dip well, numerous possible predictor variables were determined using nationally available data sources, which included information about land cover, ditch network, protected areas, topography, peatland characteristics and climatic boundary conditions. We applied boosted regression trees to identify dependencies between predictor variables and dip well specific long-term annual mean water level (WL) as well as a transformed form of it (WL_t). The latter was obtained by assuming a hypothetical GHG transfer function and is linearly related to GHG emissions. Our results demonstrate that model calibration on WL_t is superior. It increases the explained variance of the water level in the sensitive range for GHG emissions and avoids model bias in subsequent GHG upscaling. The final model explained 45 % of WL_t variance and was built on nine predictor variables that are based on information about land cover, peatland characteristics, drainage network, topography and climatic boundary conditions. Their individual effects on WL_t and the observed parameter interactions provide insights into natural and anthropogenic boundary conditions that control water levels in organic soils. Our study also demonstrates that a large fraction of the observed WL_t variance cannot be explained by nationally available predictor variables and that predictors with stronger WL_t indication, relying e.g. on detailed water management maps and remote sensing products, are needed to substantially improve model predictive performance.

HESSD
11, 3857–3909, 2014

1 Introduction

Greenhouse gas (GHG) emissions from organic soils can be high compared to mineral soils. In Germany, the fraction of organic soils classified as peatlands covers only 5 % of the land surface, but does account for 40 % of GHG emissions in the reporting categories "agriculture" and "land use, land use change and forestry" of the UN Framework Convention on Climate Change (UNFCCC) (UBA, 2012). Also other organic soils with a lower soil organic carbon content (SOC) but still meeting the definition of organic soils according to IPCC (2006) are important sources of persistently high GHG emissions (Leiber-Sauheitl et al., 2014). In our study, we also consider these soils. For simplification, we will refer in the following to the total of peatlands and "other organic soils" as organic soils. Current estimates of GHG emissions from organic soils are fairly uncertain and reporting of most countries relies on IPCC default emission factors (EF) for CO_2 emissions which are stratified for land use and climatic region, e.g. 10 t C ha^{-1} yr^{-1} for arable land in the warm temperate zone.

Artificial drainage turned the function of former natural peatlands from a C sink into a C source. Experimental work with organic soils during the last two decades showed that the aerated soil pore space above the water level is one of the key variables explaining the amount of CO_2 emissions (Moore and Dalva, 1993). Frequently, the water level relative to soil surface (further simply referred to as "water level", with negative values below ground) is used as proxy for air-filled porosity, given the simplicity and availability of water level measurements. Additionally, low water levels and oxygen availability are also key drivers of nitrous oxide (N_2O) production in organic soils (Regina et al., 1996), which increases the relevance of organic soils for climate change mitigation policy. During anaerobic conditions when water levels are at or above the land surface, substantial methane (CH_4) emissions can occur (Levy et al., 2012).

It is postulated that the GHG-budget – the sum of the CO_2-equivalents of the three main greenhouse gases (CO_2, N_2O, CH_4) – is at minimum for annual mean water levels (annual mean further defined by the variable name WL) at about −0.05 to −0.1 m

HESSD
11, 3857–3909, 2014

(Drösler et al., 2011). Following atmospheric sign convention, a positive budget stands for net emissions, while a negative sign indicates a net uptake of GHGs. Other parameters, as physical and chemical soil properties and vegetation, also influence the amount of the emissions, and thus weaken the relation between total GHG budget and WL.

If available, information about the spatial distribution of WL can identify GHG hot spot regions and improve the accuracy of total GHG budgets at large scales. The application of transfer functions that relate GHG emissions to WL and potential other influencing site characteristics can refine the estimates derived from simple application of IPCC default EFs. However, in many countries and regions, as e.g. Germany and Europe, a map of WL in organic soils does not exist. The spatial availability of measured WL is much higher than of measured GHG fluxes, which suggests the use of WL as scaling parameter for upscaling GHG emissions.

Several methods were applied in the past to produce WL maps. Their suitability is strongly related to data availability, which very often decreases in quality and spatial density with increasing scale of the study area. Spatially-distributed process-based modeling (Thompson et al., 2009) and semi-physical statistical approaches (Bierkens and Stroet, 2007), are well able to reproduce water level dynamics in wetlands environments, including peatlands. However, they heavily rely on spatial information about the system's physical properties and boundary conditions (peat hydraulic properties, hydraulic conductivity of peat base, drainage system); data that is often only available with sufficient detail at a regional scale (Limpens et al., 2008). Despite this difficulty there are studies in which process-based models were applied to model peatland water level at large scale (national or continental). Gong et al. (2012) adopted a common SVAT model to account for the differing hydrological processes in pristine fens, pristine bogs and drained peatlands, and modeled water level fluctuations in boreal peatlands for whole Finland. However, calibration and validation with data from only three mires does not allow conclusions about the accuracy and general applicability of the model. Numerous large scale hydrological wetland models are often developed with a focus

HESSD
11, 3857–3909, 2014

on delineating wetland extent (Melton et al., 2013). TOPMODEL-based schemes (Ju et al., 2006) and more advanced large scale hydrologic frameworks (Fan and Miguez-Macho, 2011) are suited to model WL, but do not account for anthropogenic drainage and thus are only applicable to pristine (or nearly-pristine) peatland systems.

When detailed physical model input that is needed for a physically-based approach is lacking, statistical or machine learning tools represent a promising alternative (Finke et al., 2004). Potential predictor variables that are available at the final map scale are determined for each location with water level data and the algorithm identifies dependencies between potential predictors and target variables, as WL or other statistical values that describe water level dynamics. For areas rich in water level data, e.g. the Netherlands, residuals of the statistical model can afterwards be analyzed for spatial correlation. If this is present, it can be used to correct for spatially correlated model bias by kriging. This scheme has been applied to agricultural areas by Finke et al. (2004) and to nature conservation areas by Hoogland et al. (2010). Spatial interpolation approaches can include ancillary data like mapped geophysical parameters (Buchanan and Triantafilis, 2009). Statistical approaches strongly rely on both quantity and quality of the data on the target variable itself, i.e. the water level data. An important quality criterion for water level data from organic soils is the measurement depth. It is crucial that there is little or no hydraulic resistance by a low conductive layer between the perforated part of the monitoring well and the fluctuating water level. If the hydraulic resistance is too high, the monitoring well acts as a piezometer and water levels may substantially differ from the actual phreatic level as shown for peatlands by van der Gaast et al. (2009). If such piezometer data is part of a dataset and interpreted as phreatic water level data during model calibration, this can lead to an under- or overestimation of predicted water levels in organic soils. An underestimation of water level predictions (too dry) is discussed for Dutch modeling studies in van der Gaast et al. (2009).

At present, in Germany a map on water levels in organic soils that could be used for GHG upscaling is missing. This and current efforts on improving GHG emission estimates for German organic soils were the main drivers for our study. Thus, the major

HESSD
11, 3857–3909, 2014

goal of this study was the development of a model concept that produces a water level map at the scale of all organic soils in Germany that is specifically optimized for water level ranges to which GHG emissions react sensitively. In a first step, we compiled a new dataset of phreatic water level time series of organic soils with contributions from numerous data providers. Based on this data, we developed a modeling approach for the annual mean water level that follows the basic idea of the statistical regionalization presented in Finke et al. (2004). However, the data situation of our study substantially differed from their study. Our data covers only a small fraction of the peatlands of the final map and spatial interpolation of residuals was not possible. We thus extended their approach by:

- including additional possible predictor variables,
- using boosted regression trees as modeling tool to identify the influence of both numerical and categorical variables simultaneously,
- applying an objective weighting scheme that balances out heterogeneous water level datasets with highly variable spatial data density,
- transforming the annual mean water level, WL, into a transformed annual mean water level, WL_t, that shows a linear relationship with the GHG budget and optimizes model calibration for the WL range relevant for GHG emissions, and by
- restricting the water level regionalization to phreatic water levels of organic soils.

We present a detailed analysis of the influence of the individual predictor variables on water levels of organic soils as well as their interactions. Furthermore, the manuscript includes the estimation of model uncertainty and possible paths of future model improvement. Finally, the calibrated model is used to derive a map of WL_t for all organic soils in Germany, and the regionalization results are presented.

HESSD
11, 3857–3909, 2014

2 Dataset and methods

2.1 Dataset of phreatic water levels in organic soils

Available data of phreatic water levels in organic soils are scarce. In contrast to data of rather deeply drilled observation wells of official groundwater monitoring networks, short peatland observation wells of only one or two meter length that measure the phreatic water level of the peat layer are currently not collected in central data management systems in Germany or any of its Federal States. With a comprehensive questionnaire started in 2011, we collected water level time series of organic soils from local agencies, non-governmental organizations, universities, consultants and other sources, and combined this data with water level data from our projects. Time series included manual and automatic measurements. Years with less than six measurements or data gaps of more than three months were excluded. Water level time series of each dip well were visually checked on plausible dynamics by comparing with data from neighboring dip wells and weather data time series. Based on auxiliary data and local knowledge, we further identified dip wells that reached down to the underlying aquifer. If dip wells failed these quality checks, they were removed from the dataset.

The final dataset comprised 7155 years of data from 53 German peatlands and 1094 dip wells. On average time series ranged over 7 years. All time series were collected at some period between the years 1988 to 2012. Data are well distributed over most of the German peatland regions and cover the three major types of organic soils (Fig. 1). Compared with the distribution of the types of organic soils in Germany, the fraction of dip wells on bogs is overrepresented in the dataset by the factor of 2.5, while dip wells on fens and other organic soils are slightly underrepresented. Data also cover the common land use types (for data sources see Table 1). However, dip wells on organic soils that are neither used for agriculture, forestry or peat mining, further referred to as “unused peatlands”, are overrepresented in the dataset by a factor of 6 as data was collected more frequently and in higher spatial data density in the frame of conservation projects. The fraction of unused peatlands of the German organic soils is

HESSD
11, 3857–3909, 2014

6 %, and the fraction in the dataset is 36 %. In contrast, dip wells on arable land are underrepresented in the dataset by a factor of 6. The fraction of arable land on German organic soils is 24 %, and the fraction in the dataset is 4 %. The other two key land use types on organic soils in Germany, grassland and forest, are well represented in the dataset. The misbalance of the land use types in the dataset is accounted for in the weighting of data (see Sect. 2.3.3).

If land use changed within the measurement period of a dip well, the time series was split at the moment when the land use record indicates the transition. For each segment the annual mean water level, WL (here with negative values defined as water levels below ground), was calculated as multi-year average value over the whole measurement period of the specific land use.

The primary application of the WL map produced in this study is for the upscaling of long-term GHG emissions as emission reporting may only reflect anthropogenic effects, but no inter-annual climatic effects. As GHG transfer functions are developed on annual data, their application requires both the long-term annual mean water level, as well as its inter-annual variability. Due to the non-linear dependence of GHG emissions on WL, single years with extreme water levels can strongly influence long-term average GHG fluxes. This study is focused on the regionalization of the long-term annual mean water levels. For this objective, model building should be based on long-term water level time series to average out the effect of weather variation within a complete climatic period (commonly 30 years). The existing nationally available data on water level time series of organic soils, however, does not comprise a single time series with complete data coverage over the last 30 years. Due to the lack of sufficient long-term water level time series, we included all time series in the model building process. Average climatic boundary conditions (precipitation, reference evapotranspiration, water balance) of the specific measurement period of each dip well are part of the predictor variables (see Sect. 2.2), and thus are supposed to partly account for the effect of specific weather conditions on WL in case of short measurement periods.

HESSD
11, 3857–3909, 2014

2.2 Predictor variables

Spatial coverage of phreatic water level data of organic soils is too low to obtain WL maps by simple spatial interpolation (Fig. 1). Additional spatial data is needed as basis for regionalization. Ancillary information that covers fully or at least most of the extent of the final map is necessary as predictor variables. A comprehensive set of variables (numerical and categorical) with potential indication for the hydrological condition of an organic soil were determined for each dip well (Fig. 2 and Table 1). This ancillary information does not necessarily need to fully cover the total map extent, as the applied machine learning algorithm in this study (boosted regression trees, see Sect. 2.3) allows for data gaps. However, the contribution to the final model decreases with increasing number of gaps in the predictor variable.

The predictor variables, which can partly be fined also in Finke et al. (2004), can be divided into seven groups:

2.2.1 Land cover

As certain land use and vegetation requires and reflects certain WL, such information can be used as indicator for average drainage level around the dip well. Land use and vegetation information was based on the German Digital Landscape Model (ATKIS Basis-DLM), which is updated continuously by aerial photos as well as sporadic ground mapping and has a temporal accuracy of 3 months to 5 years. It is provided as fine-scaled polygons and represents the best uniform land cover information available in Germany. It contains information on primary land use type, few optional vegetation attributes and whether "wet soil" has been observed during mapping. As we noticed that the use of a large number of categorical variables lowers the performance of boosted regression trees, we further aggregated the three information types (i) land use, (ii) vegetation and (iii) wet soil into a set of nine combined land cover classes (Table 1). These land cover classes were a trade-off between fine differentiation and the number of replicates in each class. For grasslands, a "wet grassland" class was separated,

HESSD
11, 3857–3909, 2014

when grassland was overlaid with wet soil and/or tree or shrubs vegetation, which may indicate a less intensive management. Forests overlaid with wet soil were separated as “wet forest”. Further, unused peatlands overlaid with wet soil and showing no coverage with any tree or shrubs attribute were characterized by higher water levels and were thus separated as “wet unused peatland”. The very few dip wells classified as open water ($n = 2$) and peat cutting ($n = 5$) were merged to the reed and arable land cover class, respectively. Land use type and land cover class were extracted at the dip well (point extraction) and as fractions in various buffers around the dip well (Table 1). As using too many weak predictor variables lowers model performance and increases overfitting, the numerous land cover fractions were further aggregated into two classes: the fraction of dry (arable and grassland, influence of the latter reduced by the factor 0.5) and wet (reed, wet grassland, wet forest, and wet unused peatland) land cover on organic soils.

2.2.2 Drainage network

Locations of ditches that are included as lines in the Digital Landscape Model were used to obtain information about the drainage network. The total length of ditches was calculated for various buffer sizes. Further, the distance to the next ditch was calculated for each dip well. A short distance to the next ditch may indicate either lower or higher water levels, depending on whether the ditches are used for drainage or already blocked and used for rewetting measures. Similarly, the indication of total length of ditches is not unique. Therefore, we defined two different sets of ditch variables. A first set, for which we calculated values for all land cover classes and a second one, for which we only calculated values for land cover classes for which ditches are undoubtedly used for drainage, i.e. arable and grassland.

HESSD
11, 3857–3909, 2014

2.2.3 Peatland characteristics

The geological map of Germany (scale 1 : 200 000) defined the area for which WL predictions were modeled. It is also the basis for topological peatland predictor variables, i.e. the fraction of organic soils in different buffer sizes as well as the dip well distance to the edge of the peatland. Information about the peatland type and the substrate at the peat base is presented in more detail in a newly compiled raster map of organic soils (Fell et al., 2014) and was thus extracted from this map. Peatland types were aggregated into five classes: lowland bog (North German Plains and Alpine Forelands), upland bog (Central Uplands and Alps), fen neighboring surface water, fen without neighboring surface water, and a class of "other organic soils" that do not fulfill the C content and thickness criteria to be classified as peatland.

2.2.4 Climatic boundary conditions

Climatic boundary conditions directly influence water level. On the one hand, the typical long-term climatic boundary conditions may indicate the general vulnerability of peatlands in a specific region. On the other hand, given the different lengths of measurement periods of the time series in this study, climatic boundary condition predictor variables may account for the effect of a climatically wetter or drier measurement period, compared to the long-term averages, on the water level. Climatic boundary conditions were extracted from a 1 km × 1 km raster of the German Weather Service. Annual, summer and winter precipitation, FAO56 Penman-Monteith reference evapotranspiration, and climatic water balance (difference between precipitation and reference evapotranspiration) were determined for the individual measurement period of each dip well and as long-term averages (30 years).

HESSD
11, 3857–3909, 2014

2.2.5 Relative altitude

Relative altitude was calculated by subtracting the median altitude of various buffer sizes from the absolute altitude at each dip well in the DEM. Relative altitude is expected to have two different indications depending on the applied buffer size: (i) In many peatlands, the former smooth peatland relief at the scale of approximately > 5 m has been disturbed due to peat cutting and differences in drainage and mineralization rate. As a consequence, the rather smooth phreatic surface often does not follow the uneven and patchy terrain. Relative altitude with respect to smaller buffer sizes (< 250 m) may therefore explain part of the WL variation, e.g. a dip well that is located at a surface much higher than the surrounding may indicate deeper water levels; (ii) for large buffer sizes (> 250 m) relative altitude indicates whether the peatland lies in a larger morphological depression or elevation, and thus may indicate whether large scale lateral inflow of water can be expected or not. Similar indication is provided by the topographic index (see below). The accuracy of relative altitude values depends on the resolution and accuracy of the DEM. The nation-wide available DEM is based on datasets of varying quality, which may lower the influence of this variable.

2.2.6 Topographic wetness index

The topographic wetness index is a common wetness indicator used in hydrology (Beven and Kirby, 1979). It is a combined measure of catchment area and slope at a given point and indicates the extent of flow accumulation. It was calculated for various DEM resolutions using the GRASS 7 module r.watershed.

2.2.7 Protection status

The protection status of a peatland area may reflect hydrological conditions. Therefore we checked for seven protection status at each dip well (see Table 1 for details).

HESSD
11, 3857–3909, 2014

2.3 Model building scheme

Model building was performed using boosted regression trees (BRT), implemented in the two R packages "gbm" (Ridgeway, 2013) and "dismo" (Hijmans, 2013). BRT is a machine learning algorithm, in which the final model is derived from the data. Functions that relate target to predictor variables are not predetermined but freely developed. BRT modeling is increasingly applied in spatial modeling of species or numerical environmental variables (Elith et al., 2008; Martin et al., 2011), thereby often showing superior performance compared to other machine learning algorithms. The increasing application of BRT is related to several of its favorable characteristics: the strength of this method lies in the ability to fit complex functional dependencies including non-linear relationships and interactions between predictor variables. Based on its flexibility, BRT is invariant to monotonic transformations of predictors. Furthermore, BRT allows missing values, is fairly insensitive to outliers and can estimate the relative contribution of each predictor variable to the model. Due to these characteristics we expected BRT to be very well suited for the very heterogeneous dataset of this study.

BRT modeling is based on the decision tree concept, with the major difference that each decision tree has a reduced learning rate. Thus, the final model consists of thousands of overlapping decision trees, similar to the ensemble approach. BRT model calibration is prone to overfitting, and there are several ways to reduce this behaviour. Due to the overfitting behaviour, cross validation is generally part of the model building process. However, cross validation can be performed in several ways and, if performed carelessly, can lead to over-optimistic model performance (De'ath, 2007). Here, cross validation was performed by leaving out whole peatland areas instead of a random set of dip wells. This represents a stricter cross validation, and we noticed that it strongly reduced overfitting of the water level data, and thus contributed to the development of a more robust model.

Another way to avoid overfitting is to impose monotonic slopes on the effects of individual parameters, which can even lead to improved prediction performance (De'ath,

HESSD
11, 3857–3909, 2014

2007). For all our numerical variables we expected monotonic slopes rather than optimum functions. To avoid predefining any expected direction, all numerical variables were added twice to the set of predictors, constraining the slope to a monotonic increase and decrease. We let the model decide whether monotonic increase or decrease has higher predictive power.

Models were calibrated using a Gaussian response type, aimed at minimising deviance (squared error) (Ridgeway, 2013). In all calibration runs, we applied the gbm.step function of the dismo package, which assesses the optimal number of boosting trees using cross validation. We tested various learning rates (0.001–0.01), bag fractions (0.1–0.8) and levels of tree complexity (3 to 7), i.e. the number of nodes in a tree. By trial-and-error we determined the most effective algorithm parameters for our dataset being 0.005 for the learning rate, 0.6 for the bag fraction and 5 for the tree complexity.

The final BRT model building is commonly performed as a two-step procedure (Elith et al., 2008) which we basically also followed in our study: (i) in the first step, the whole set of predictor variables is used to calibrate a BRT model. (ii) In a second step, the number of parameters is reduced sequentially to avoid overfitting and to derive a more parsimonious model. We tracked predictive performance criteria during the simplification process. As various variables were calculated for different buffer sizes, our predictors included a large number of correlated variables. Correlation coefficients between predictor variables of > 0.7 are known to severely distort model estimation and subsequent prediction (Dormann et al., 2013). Thus, we performed this simplification process by first dropping those parameters with a correlation > 0.7 (either Pearson or Spearman type) to another parameter with a higher contribution (Clapcott et al., 2011). This avoided that two highly correlated parameters remain in the parameter set longer than the last parameter of another group of variables, which may contribute less compared to the two highly correlated parameters but provides extra information that is not covered by the other parameters. After all highly-correlated parameters have been dropped, further parameters with low contribution were dropped progressively.

HESSD
11, 3857–3909, 2014

Predictor contributions are calculated as proportional contributions to the total error reduction, and can be considered as a measure for the influence of the individual predictors. Additionally, a BRT model allows to derive partial dependence plots which indicate how the response is affected by a certain predictor after accounting for the average effects of all other predictors in the model (Elith et al., 2008). These plots do not show the full effect of each parameter on the model response due to interactions with other parameters that are fixed to derive theses plots as well as due to parameter co-correlation. However, they can be used for interpreting model behavior (Elith et al., 2008).

2.3.1 WL_t: transformation of WL

The map of water levels of this study was developed to improve the upscaling of greenhouse gas emissions from organic soils. Therefore, the final map should provide the highest accuracy for the water level range for which the highest differences of greenhouse gas emissions occur. This can be achieved by transforming WL into a transformed variable WL_t, which shows linear relationship with GHG emissions. The sensitivity of greenhouse gas emissions to water level has been analyzed in several laboratory and field experimental and monitoring studies (Berglund and Berglund, 2011; Drösler et al., 2011; Hahn-Schöfl et al., 2011; Leiber-Sauheitl et al., 2014; Moore and Dalva, 1993; Moore and Roulet, 1993). General trends are a strong increase of methane (CH_4) emissions for annual mean water levels of approximately > -0.1 m and an increase of CO_2 emissions for water levels < -0.1 m with a trend similar to a saturation function that levels out approximately between -0.4 and -0.8 m (Fig. 3a). While studies agree over these general trends, the exact shape of the transfer function and the maximum levels of emissions as well as their dependence on soil properties and other environmental parameters are still discussed controversially. Here, we assume a hypothetical transfer function, relating the normalized GHG budget, ranging from 0 to 1, to the water level (see also Fig. 3),

HESSD
11, 3857–3909, 2014

$$\text{GHG Balance} = \begin{cases} -e^{3(\text{WL}+0.1)} + 1 & \text{WL} \le -0.1 \\ 1 - e^{-3(\text{WL}+0.1)} & \text{WL} > -0.1 \end{cases}. \quad (1)$$

As GHG budget can be positive for both low and high WL, we introduced the transformed water level, WL_t, as (Fig. 3),

$$\text{WL}_\text{t} = \begin{cases} e^{3(\text{WL}+0.1)} - 1 & \text{WL} \le -0.1 \\ 1 - e^{-3(\text{WL}+0.1)} & \text{WL} > -0.1 \end{cases}. \quad (2)$$

By calibrating the model to both WL and WL_t, we test whether optimization on WL_t provides highest model accuracy for the water level range relevant for GHG emissions and whether it optimizes the map for application to GHG upscaling.

2.3.2 Model performance criteria

Model fit and predictive performance after cross-validation were quantified by the weighted root mean square error,

$$\text{RMSE} = \sqrt{\frac{1}{\sum w_i} \sum_{i=1}^{m} \left(w_i \left(x_\text{o}^i - x_\text{s}^i \right)^2 \right)}, \quad (3)$$

where m is the number of dip wells, x_o^i is observed WL or WL_t of dip well i and x_s^i is simulated WL or WL_t of dip well i, and w_i is the data weight of dip well i (see below). We refer to the root mean square error of the predicted data of cross validation by RMSE_cv. Model performance was further quantified by Nash–Sutcliffe Efficiency (NSE),

$$\text{NSE} = 1 - \frac{\sum_{i=1}^{m} w_i \left(x_\text{o}^i - x_\text{s}^i \right)^2}{\sum_{i=1}^{m} w_i \left(x_\text{o}^i - \overline{x_\text{o}} \right)^2}, \quad (4)$$

HESSD
11, 3857–3909, 2014

where $\overline{x_0}$ is the mean of all observed WL or WL_t. It indicates how well observed vs. predicted values match the 1 : 1 line. NSE is a good overall indicator of predictive performance because it combines scatter and bias (common offset and/or slope difference from 1 : 1 line) (Nash and Sutcliffe, 1970). Values greater than 0 signify a model that is better than the reference model based on the data mean. We refer to the NSE of the training data by NSE_{cal}, and of the predicted data of cross validation by NSE_{cv}.

Systematic errors were quantified by calculating the model bias, here defined as,

$$\text{BIAS} = \sum_{i=1}^{m} \left(w_i x_o^i - w_i x_s^i \right).$$

2.3.3 Weighting scheme

The dataset contains peatland areas that strongly differ in their spatial extent and in the number of installed dip wells. To use the information in the data in an optimal fashion, it is important to introduce a weighting of the data. Without data weighting during calibration, too much influence is given to small and highly equipped peatlands, which reduces predictive model performance for large less well equipped peatland areas. To avoid this in a simple manner, weight could be reduced by the number of dip wells in each peatland, which results into each peatland being equally weighted. This scheme however does not sufficiently use the high information content provided by highly-equipped large peatlands, which should have a higher impact on model calibration than a small peatland with only few dip wells. Here, we present an objective weighting scheme that takes into account both factors, peatland size and local density of dip wells, to derive dip well specific weighting factors.

A common way to introduce individual data weights is to use the inverse of the error variance σ_e^2. For dip well i the weight is:

$$w_i = \frac{1}{\sigma_{e,i}^2}. \quad (5)$$

HESSD
11, 3857–3909, 2014

Let us consider the extreme case that there are two dip wells separated by only a few meters, so they are basically totally correlated regarding their water level dynamics. The absolute water level, however, may differ between the two dip wells due to micro-topography and measurement error. The second dip well can be considered as a repeated measurement. A reasonable approach would be to take the mean of both measurements and to reduce the error variance by the inverse of the square root of the number of measurements, for this example $n = 2$, which is common statistics for repeated measurements:

$$w_i = \frac{1}{\frac{1}{\sqrt{n}}\sigma^2_{e,i}}. \quad (6)$$

Instead of taking the mean of the two dip wells, it is equally possible to keep both dip wells. Then the weight of each dip must be divided by the number of fully-correlated measurements, here $n = 2$:

$$w_i = \frac{1}{n\frac{1}{\sqrt{n}}\sigma^2_{e,i}}. \quad (7)$$

Dip wells that represent only "partly repeated" measurements, i.e. indicate some degree of spatial correlation, can be accounted for by analyzing the spatial correlation structure of the dataset. Here, we fitted a single spherical variogram model to the sample variogram of all data (Fig. 4 in Sect. 3.1). The variogram model provides a nugget, a sill, and a range of spatial correlation for the given dataset of WL. The fraction of spatial correlation, i.e. the correlated data variance, can now be obtained for any distance between two dip wells i and j by:

$$f_{i,j} = \frac{\text{sill-gamma}_j}{\text{sill-nugget}}. \quad (8)$$

HESSD
11, 3857–3909, 2014

Parameter n of Eq. (7) can be determined for each dip well i as the sum of contributions of all dip wells that are within the range of spatial correlation:

$$n_i = 1 + \sum_{j=1}^{m} \frac{\text{sill-gamma}_j}{\text{sill-nugget}}, \quad (9)$$

where gamma_j is calculated based on the variogram parameters and the distance between dip well i and j. Only dip wells with the same land use type were summed up with Eq. (9), which avoids the down-weighting of dip wells with different land use type. The latter are mostly characterized by fairly different WL, thus by rather low spatial correlation to dip well i.

After spatial correlation has been accounted for, the sum of the weights of all dip wells of each land use type were adjusted that they correspond to the fractions of this land use type in Germany. This adjustment accounts for the overrepresentation in the dataset of dip wells in unused peatlands and underrepresentation of dip wells in arable land.

2.4 Model uncertainty and stability evaluation

Uncertainty of the model predictions was assessed by bootstrapping, cross-validation and residual analysis.

For the bootstrapping analysis, we followed the procedure of Leathwick et al. (2006). We estimated the confidence intervals around the predictions and the fitted functions by taking 1000 bootstrap samples of the 53 peatlands. The number of peatlands in each sample was equivalent to the dataset, but peatlands were selected randomly with replacement. Using the predictor variables of the final model, a BRT model was fitted to each sample. Cross validation was again performed on peatlands, thus a peatland in the calibration dataset was not part of the cross-validation dataset to avoid over-optimistic results. Variances of the predictions and of the fitted functions of the 1000 models were evaluated.

HESSD
11, 3857–3909, 2014

If datasets are relatively small (e.g. $n < 1000$; De'ath, 2007) then the small size of the training and test datasets lowers model accuracy. Given the fairly small number of peatlands in the dataset and the partly high spatial correlation of dip wells within these peatlands, we decided not to split the dataset into a training and test dataset. Estimates of model accuracy can then be based on cross-validation, thereby making effective use of all the data (De'ath, 2007). The prediction uncertainty of the final model is estimated by the root mean square error of prediction ($RMSE_{cv}$, see above) for each land cover class. After testing for normal-like distribution of the residuals, $RMSE_{cv}$ can be used to derive the 68 and 95 % confidence intervals of the predictions with $RMSE_{cv}$ and $2 \times RMSE_{cv}$, respectively.

Finally, additional residual analysis was performed to evaluate whether the predictions are biased for different land cover classes or geographical regions.

2.5 Regionalization

In the final regionalization step, the predictor variables contributing to the final model were determined at a 25 m × 25 m raster for all organic soil in Germany. Predictor variables were determined with the same map input that was used for model building. Land cover information including information on ditches was based on the data from year 2012 and the climatic data was based on the average of the last 30 years. The fine spatial resolution of 25 m × 25 m was not chosen to fool the reader with a spatially highly accurate model. But, this fairly fine scale was necessary to map the relatively small scale effects of the topography, land use and peatland geometry variables. The final model was then used to make a prediction for each of these raster cells.

HESSD
11, 3857–3909, 2014

3 Results and discussion

3.1 Spatial correlation structure of the dataset

The variogram model fitted to the sample variogram provided a nugget (0.012 m^2; 0.11 m), a sill (0.09 m^2; 0.3 m), and a range of spatial correlation (2700 m) for our dataset of WL (Fig. 4). The nugget represents the very small-scale soil hydraulic variability and micro-topography effects on WL (van der Ploeg et al., 2012) and measurement error, e.g. by differences in the determination of the ground surface and in the timing of the manual measurements. Furthermore, micro-topography (e.g. hummocks) and oscillating peat surfaces of wet peatlands pose a challenge for an accurate determination of both ground surface and water level. The water level time series in the dataset were of different lengths and ranged from 1 to 20 years. Interannual variability of water levels can be large (e.g., Knotters and van Walsum, 1997). For simplicity, in our analysis, data were not harmonized by extrapolating WL time series using weather data to a 30 year period. Thus, the nugget also includes errors that are introduced by dip wells with different measurement periods that are located in the range of spatial correlation. In consideration of these error sources, the fitted nugget of 0.11 m appears to be a realistic value. The fitted sill matched with 0.3 m nearly perfectly the standard deviation of the data (0.31 m), which indicates consistency between semivariogram model and dataset. The fitted range of spatial correlation of 2700 m reflects both physical effects, i.e. the average range of lateral flows due to hydraulic gradients, as well as the effect of average land use patterns in Germany on spatial correlation of WL. Fitted values were used in the calculation of the dip-well specific weights using Eqs. (7) and (9).

3.2 Typical water levels for land use types in German organic soils

The land cover classes are characterized by plausible mean and median water levels, which show consistent differences among each other (Table 2 and Fig. 5a). The mean

HESSD
11, 3857–3909, 2014

values of arable land and grassland agree with what can be expected for their agronomic requirements, with slightly lower water levels for arable land. The high variability observed for both classes may be related to the variability of the efficiency of installed drainage systems, as e.g. the presence and condition of tile drains and the depth of ditches. Grasslands can be managed with very variable intensity, which is partly reflected in different water levels. Figure 5a further shows that deciduous forests seem to dominate on slightly drier organic soils compared to coniferous forests, which dominate under wetter conditions. A high variability of water levels is observed for the land cover class "unused peatland". On the one hand, post peat-cutting topography increases the variability of WL over short distances. It probably contributes to the high variance observed for this class. On the other hand, this class comprises both rather dry unused peatlands and wetter peatlands in which re-wetting measures already took place, which however do not show yet a "wet soil" attribute in the ATKIS Digital Landscape Model. This may also cause part of the variance observed in the grassland and forest land cover class. All "wet" land cover classes (reed, wet grassland, wet forest, and wet unused peatland) that were separated by wetness indication clearly show higher water levels, showing the wetness attribute of the Digital Landscape Model is a useful attribute.

Figure 5b shows the transformed water level for all classes. It can be observed that the variances of the wetter land cover classes relatively increase compared to the variances of the dry land cover classes. This is due to the highest sensitivity of GHG emissions in the wet range of water levels (> -0.5 m). Consequently, the rather high variance of WL for arable land corresponds to a rather low variance of WL_t, i.e. to a rather low assumed effect of WL variability on the GHG budget.

3.3 BRT model calibration and validation: WL vs. WL_t

In contrast to land cover class, the other predictor variables showed, if at all, only weak relations to WL and WL_t when evaluating them with box plots, 2-D cross plots and

HESSD
11, 3857–3909, 2014

simple correlation matrices. Here, we expected BRT to detect the strongest predictor interactions and to identify the most informative predictors.

After model calibration with all predictors, subsequent model simplification successively dropped those parameters with correlation > 0.7 and lowest contribution. For both, WL and WL_t, model performance improved during this simplification. For WL_t, highest values of NSE_{cv} of approximately 0.46 were achieved with 21 to 9 model parameters. The development of NSE_{cv} for the last 50 parameters is shown in Fig. 6. Further elimination of parameters led to a pronounced decline of model performance. Similar behavior was observed for the calibration on WL. In favour of a more parsimonious model we chose the model with the lowest number of parameters before the pronounced decline of model performance occurred. For the calibration on WL_t, this corresponded to the model with lowest number of parameters that still achieved NSE_{cv} values of > 0.45 (Fig. 6). The final WL_t model comprised nine predictor variables, and the final WL model seven parameters. The percentages of parameter contributions to the final model and their individual influences are discussed for WL_t in Sect. 3.4.

Table 3 summarizes the statistical performances of the models calibrated on WL and WL_t. For both models NSE_{cal} is considerably higher than NSE_{cv} and shows the commonly observed overfitting behavior of BRT models. The different measures that we conducted to minimize overfitting (cross-validation on peatlands, restriction to monotonic responses, and model simplification including elimination of highly correlated variables) lowered the difference between NSE_{cal} and NSE_{cv} but could not totally avoid overfitting. NSE_{cv} of the WL_t model (0.453) indicates higher predictive model performance compared to the WL model (0.381). However, as the data ranges differ due to the transformation, this comparison may be misleading. Therefore, we transformed the predictions of the WL model to obtain WL_t values from this model and equally calculated the performance criteria (Table 3, second column). Then, NSE_{cv} is slightly increased (0.397), but does not achieve the values of the model that was calibrated on WL_t. A better predictive model performance of the model calibrated on WL_t is also visible for the $RMSE_{cv}$ values. The total $RMSE_{cv}$, as well as the $RMSE_{cv}$ values for the

HESSD
11, 3857–3909, 2014

dry (WL < −0.3 m) and wet range (WL > −0.3 m), show slightly lower values for the WL_t model compared to WL_t values from the model calibrated on WL. Given our hypothetical transfer function (Fig. 3) in which the GHG budget is linearly related to WL_t, the higher accuracy of WL_t predictions directly corresponds to a higher accuracy of GHG budget predictions.

Superior model performance is also evident when evaluating model bias. Only when calibrating directly on WL_t, the WL_t predictions are bias-free. Calibration on WL and subsequent transformation to WL_t, introduces a model bias towards systematically lower WL_t values. In subsequent applications to GHG emission upscaling, lower WL_t values would lead to an overestimation of CO_2 emissions and to an underestimation of CH_4 emissions.

3.4 Influence of predictor variables on WL_t

Given the beneficial characteristics of the model calibrated on WL_t for GHG upscaling, presentation and discussion of further model results is restricted to the WL_t model.

The BRT method allows to analyze the parameter contributions to and influences on the model (Elith et al., 2008) and thus may contribute to the system understanding. The percentages of the contributions of the nine predictor variables to the final model ranged from 25.2 to 5.6 % (Fig. 7). Except of protection status, at least one parameter of each of the seven parameter groups contributed to the final model. All protection status information was dropped early during the simplification process due to low contribution, although WL showed slightly higher values for data from Nature Protection or Special Areas of Conservation. However, other parameters seem to be able to fully compensate the information that is lost by dropping this predictor.

Land cover class, lc, at the dip well was the parameter with strongest contribution (25.2 %). It basically follows the trend illustrated in Fig. 5b. The bootstrap error plotted as standard deviation (Fig. 7) shows the variation of this influence over the 1000 bootstrap models. A second land cover parameter, the fraction of dry land cover classes on organic soils in a buffer of 2500 m radius, $f_{dry}(2500)$, contributed to the model with

HESSD
11, 3857–3909, 2014

10.3 %. The monotonic decrease of WL_t with increasing $f_{dry}(2500)$ is plausible, as higher values reflect intensive land use in the surroundings of the dip well and thus indicate intensive artificial drainage. Together both parameter contributed by 35.5 % and thus land cover represents the parameter group with the strongest model contribution.

Peatland characteristics are the second most important parameter group. The peatland type contributed by 16 %. The model indicates that peatlands without any connection to surface water bodies (river or lake) and the class of other organic soils are characterized by lower WL_t compared to the peatland types lowland bog, upland bog and fen neighboring surface water. As the class of other organic soils is generally expected to reflect lower water levels and as surface water may have a stabilization effect on water levels of organic soils, the influence of the peatland type can be considered as plausible. Besides peatland type, the substrate of the peat base contributes by 5.6 %. Here, organic soils overlying limnic sediments (e.g. calcareous gyttja) or basement rock are characterized by higher WL_t compared to organic soils overlying unconsolidated rock. This can be explained by the lower drainage resistance of unconsolidated rocks. This may cause an increased efficiency of anthropogenic drainage and/or a general higher vulnerability to seepage losses. Finally, slightly lower WL_t values are indicated by a high fraction of organic soils for the 500 m buffer, $f_{peat}(500)$. This may reflect the higher land use pressure on large peatlands compared to rather small peatlands, which tentatively are more easily preserved by nature protection efforts.

The remaining four parameter groups are represented in the model by only one parameter each. The third most influential parameter was the length of ditches on arable land and grassland for the 250 m buffer, $di_{len,\,dry}(250)$. At first glance, it may be surprising that with increasing ditch density, WL_t values tend to be higher, as ditches are supposed to drain the water when land is used as arable land and grassland. The fact that the model identifies a rather strong effect in the opposite direction may be caused by the incomplete information about the drainage network. There is not detailed information about the spatial distribution of tile drains. Based on expert knowledge, agricultural

HESSD
11, 3857–3909, 2014

areas with a lower ditch density are more likely to be equipped with tile drains. As the latter, easily installed with a narrow drain spacing, are more effectively draining organic soils, low WL_t values for arable land and grassland may be related to low ditch densities. Furthermore, ditches were originally dug at narrow spacing in especially wet areas of organic soils, but there is no information available whether these ditches still function properly.

The parameters wb_{summer}, h_{rel} and ti_{ras25} all show expected trends. The model predicts higher WL_t for increasing climatic water balance in the summer period (May to October), wb_{summer}, and for dip wells located in depressions (low values of h_{rel}), and for higher small-scale topographic wetness indices calculated on the 25×25 digital elevation model (ti_{ras25}).

The fact that all parameters show expected or explainable responses in the model corroborates the reliability of the calibrated WL_t model. The standard deviation of the predictor responses based on the bootstrap samples shows the stability of the observed responses.

Further insights into model behavior can be obtained by analyzing parameter interactions. This is obtained by changing two parameters simultaneously while keeping mean values for all other parameters (Elith et al., 2008). Figure 8 shows the two strongest parameter interactions. Parameter wb_{summer} strongly interacts with p_{type}. The generally lower values of WL_t of fens without surface water connection and other organic soils show a stronger dependency on the summer climatic water balance. While a summer climatic water balance of > -80 mm shows rather low further effect on WL_t for the wetter peatland types, in contrast for the two drier peatland types there is still a strong effect with increasing wb_{summer}. The trend for $wb_{summer} > 130$ mm for the dry peatland types is supported by seven different peatlands.

Another strong interaction is observed for p_{base} and $f_{dry}(2500)$. While a rather low effect of the fraction of arable land and grassland is observed for organic soils overlying basement rock and peat clay layer, strong effect is observed for organic soils overlying unconsolidated rock. This interaction reflects the higher lateral range of drainage

HESSD
11, 3857–3909, 2014

effects for organic soils with little flow resistance at the peat base. In these organic soils, intensive land use lowers water level over large areas.

3.5 Discussion of model uncertainty

Plotting observed vs. predicted WL_t from cross-validation (Fig. 9) illustrates the rather large residual variance that cannot be explained by the model. As indicated by the higher $RMSE_{cv}$ for the wet range (Table 3), scatter increases with increasing WL_t. Error bars in the *y* direction indicate data error derived from the nugget of the variogram. It is exemplarily shown for a few data points. Due to transformation, data error increases for higher WL_t. Figure 9 demonstrates that the fraction of unexplainable variance related to data error is much higher for the wet than for the dry range. Bootstrap error that indicates the variation of the model predictions for 1000 bootstrap samples is shown in the *x* direction for the same data points. Bootstrap error is lower than the data error for the wet range and slightly higher for the dry range.

Bootstrap errors demonstrate the sensitivity of model predictions to changes of the dataset used for calibration. When a model possesses structural deficits, such as missing predictor variables, bootstrap errors should not be used to define confidence intervals for the model predictions. Figure 10 shows residuals from cross-validation and standard deviation of bootstrap predictions for all land cover classes. The residuals of each land cover class show normal-like distributions. For five of the nine land cover classes (wet forest, wet unused peatland, arable land, coniferous forest, and reed), Shapiro–Wilk test of normality is positive ($p > 0.05$). Figure 10a further indicates that residuals of each land cover fairly well scatter around zero, indicating low bias for the various land cover classes. Land cover class specific confidence intervals of model predictions can thus be derived from the $RMSE_{cv}$ of each land cover class, e.g. $2 \cdot RMSE_{cv}$ representing the 95 % confidence interval.

The prediction uncertainty derived from cross-validation is much higher than the bootstrap prediction uncertainty obtained from the bootstrap standard deviation (sd), with 2*sd corresponding to the 95 % confidence interval (Fig. 10). The large difference

HESSD
11, 3857–3909, 2014

between these values indicates that the model has structural deficits that can be attributed to several error sources: (i) key influences on WL_t are missing in the set of predictor variables. None of the predictor variables indicate whether and to which extent water level increase due to re-wetting measures took place in the last years. Wetness indicators (wet soil and/or vegetation attributes) that are obtained from the Digital Landscape Model probably react with a delay of several years. Thus, we expect the occurrence of several observed high WL_t values that cannot be explained by any of the predictor variables. (ii) Small-scale topography that is not represented with sufficient detail and accuracy in the DEM may cause that several predictions strongly differ from what would be expected from the other predictor variables. A common example may be a dip well that is located on a narrow peat ridge, which remained after peat-cutting and is absent in the DEM, and that is situated in an area classified as wet soil by the Digital Landscape Model. Then, the model indicates a WL_t that is much higher than the observed WL_t, as for the observed value the reference surface was the surface of the peat ridge. (iii) Consistent information about tile drains is missing and only exists regionally (Tetzlaff et al., 2009). At the national scale, however, there are no maps on tile drains. Tile drains are known to have a strong effect on WL_t for arable land and grassland. As explained above, we expect parameter $di_{len,\,dry}(250)$ to partially compensate for this missing information. (iv) Another source of prediction uncertainty may comprise inconsistent and erroneous land cover classification of the Digital Landscape Model due to the high degree of subjectivity for many of the attributes. Furthermore, the temporal accuracy of the Digital Landscape Model may be as bad as 5 years which can cause time series with land use change to be split at the wrong date, and vegetation and wetness attributes not yet to be updated to the current conditions.

(v) The water balance of fens strongly depends on the size and the hydraulic head of the groundwater catchment. Unfortunately, there is no consistent map on hydraulic heads or groundwater catchments for all Germany.

We checked model predictions for geographical bias. Geographical location was not one of the model parameters. However, history and policy of land use on organic soils,

HESSD
11, 3857–3909, 2014

current ditch water management and climate do show large-scale geographical trends. We divided our dataset into the three major German peatland regions (NE, NW and S) and evaluated the model residuals (Fig. 11) to see whether our model is biased due to important missing geographical effects. A serious bias for any of the three major German peatland regions cannot be identified.

When applying calibrated statistical models during regionalization, it is important to check model behavior for extrapolation outside the range of the parameter space that is covered by the data upon which the model was built. BRT always extrapolates at a constant value from the most extreme environmental value in the training data. In contrast to other types of statistical models, e.g. generalized linear models, BRT does not continue the fitted trend beyond the last observation. Regarding the categorical variables, the dataset covers all classes occurring in Germany with several peatlands. The dataset also covers the major range of values occurring in Germany for the numerical predictor variables. Furthermore, Fig. 7 indicates that the constant values, at which the model extrapolates the influence of the variables, do not raise major concern for any extreme predictions outside the parameter range.

3.6 Regionalization

The map of WL_t resulting from the application of the fitted WL_t model to all grid cells shows gradients at the regional scale (Fig. 12a). E.g. in the south of Germany, a gradient from wet to dry can be observed for the pre-alpine upland bogs and the peatlands of the moraine plain. In the north of Germany, the map indicates that organic soils in the very NE are wetter than the rest. For the rest of the north a slight gradient can be observed from less dry to dry from NW to E, which is mainly driven by the higher summer climatic water balance in the NW. As both categorical and numerical predictor variables do also vary at sub-regional scale, the resulting map also shows gradients within peatland areas, e.g. due to small-scale land use ditch density gradients and topography effects (Fig. 12b).

HESSD
11, 3857–3909, 2014

We calculated WL_t averages of the land cover classes using the regionalized WL_t from the map (Table 2, column 3). The given standard deviation comprises both the variability within a land cover class that is explained by the model as well as the uncertainty of each prediction. Resulting means and standard deviations slightly differ from the corresponding values of the dataset. The land cover specific WL_t values obtained from the map can be considered as being more representative, as the regionalization procedure is supposed to partly account for potential bias in the dataset.

When applying this map and its predicted WL_t values in subsequent GHG upscaling, it is crucial that model uncertainty is propagated properly. An example demonstrates the necessity of uncertainty propagation. For a grid cell classified as wet grassland, the probability distribution of WL_t is shown based on a normal distribution that was fitted to the residuals of this land cover class (Fig. 12c). Without propagating the uncertainty and when only translating the predicted WL_t (eventually in combination with other parameters, e.g. soil properties) into a GHG budget, GHG budget is strongly underestimated as the WL_t prediction is close to zero, indicating neither large CO_2 nor CH_4 emissions. When translating the full distribution of WL_t into a GHG budget, the resulting GHG budget would be much higher, as at both sides of the predicted WL_t the GHG budget increases.

3.7 Possible paths for model improvement

The model performance that is achieved by the statistical approach presented in our study raises the question whether collecting more WL data can improve model performance or whether the factor that is constraining the model performance is the limited strength of the nation-wide available predictor variables. To assess this question, additional "holdout models" were developed by fitting the BRT model to various random sets of data with a limited number of peatland areas (from 10 to 50 peatlands). For each number of peatland areas, 500 random selections were calibrated and model performance was evaluated with NSE_{cv}. As expected, results indicate an increase of model performance with increasing number of peatlands used in the model building

HESSD
11, 3857–3909, 2014

process (Fig. 13). Results also indicate a substantial flattening of the learning curve. Thus, further collection of WL data may only lead to a substantial model improvement when including many more peatlands into the dataset. More promising would be the specific collection of more data on the weakly represented and/or important land cover classes arable land and grassland.

Another path to achieve a stronger model improvement is the development of new predictor variables. In future, the availability of a more accurate DEM based on laser-scanning data, which is already available at full coverage for some federal states of Germany, may strongly increase the predictability of the observed WL data. Additionally, a nation-wide map on water management and on the distribution of tile drains may represent great potential to explain large parts of the residual variance and/or even allow setting up a large scale physically-based model that includes water management. Furthermore, data harmonization by extrapolating the water level time series of our dataset with the climatic boundary conditions of the last 30 years may lower the unexplainable variance of the dataset due to short measurement periods (Bartholomeus et al., 2008), an effort that has been successfully conducted in Finke et al. (2004) using the transfer noise model of Bierkens et al. (1999). Finally, we believe that the inclusion of remote sensing products in our statistical model approach, as e.g. spaceborne microwave soil moisture observations (Sutanudjaja et al., 2013), may hold large potential to improve model performance as moisture differences due to varying water levels are high for organic soils.

4 Conclusions

Our study demonstrates the potential of statistical modeling for the regionalization of water levels in organic soils when data covers only a small fraction of peatlands of the final map and thus spatial interpolation is not possible. With the available dataset of target and predictor variables, it was possible to predict 45 % of the GHG relevant water level variance in the dataset in a cross-validation scheme. The variance is explained by

HESSD
11, 3857–3909, 2014

nine predictor variables. With the analysis of their effect on the water level it was possible to gain insights into natural and anthropogenic boundary conditions that control water levels of organic soils in Germany.

Based on a hypothetical GHG transfer function relating GHG emissions to annual mean water levels (WL) we showed the advantage of transforming the annual mean water level into a new variable (WL_t) to which GHG emissions linearly depend on. The transformation improved model accuracy, increased the explained variance of the water level range that is relevant for GHG emissions and avoided model bias.

The presented approach is transparent and allows successive improvement when new input data and predictor variables become available. Our results show that model improvement by increasing number of WL_t data, however, seems to be limited. If efforts are made, data collection should be concentrated in agriculturally used organic soils, for which relatively few data is available. We believe that the constraining factor of model performance is rather the weakness of the predictor variables that are currently available at large scales. The development of new more informative predictor variables, as e.g. water management maps and remote sensing products, may represent the more promising path for model improvement.

The proposed regionalization approach is suited to application to any other country when similar data on target and predictor variables is available. It is important that the spatial resolution of the predictor variables is high enough (Finke et al., 2004). If predictor variables like land use and peatland type are only available at a much coarser scale and provided as percentages for grid cells, the dependency between predictor variables and the rather local WL will be probably lost for most of the predictor variables.

Acknowledgements. Several institutions made their data available for this synthesis study. We gratefully thank ARGE Schwäbisches Donaumoos, Biologische Station Steinfurt, Biosphärenreservat Vessertal, BUND Diepholzer Moorniederung, Deutscher Wetterdienst (DWD), Bezirksregierung Detmold, Förderverein Feldberg-Uckermärkische Seenlandschaft, Hochschule für Wirtschaft und Umwelt Nürtingen (Institut für Angewandte Forschung), Hochschule Weihenstephan-Triesdorf (Professur für Vegetationsökologie), Humboldt Universität zu Berlin (Fachgebiet Bodenkunde und Standortlehre), Landkreis Gifhorn, LBEG Hannover (Referat

HESSD
11, 3857–3909, 2014

Boden- und Grundwassermonitoring), LUNG Mecklenburg-Vorpommern, Eberhard Gärtner, IGB Berlin (Zentrales Chemielabor), Landkreis Gifhorn, NABU Minden-Lübbecke, Naturpark Drömling, Naturpark Erzgebirge/Vogtland, Region Hannover, Naturpark Nossentiner/Schwinzer Heide, Naturschutzfond Brandenburg, Ökologische Station Steinhuder Meer, Technische Universität München (Lehrstuhl für Vegetationsökologie), Universität Hohenheim (Institut für Bodenkunde und Standortslehre), Johannes Gutenberg-Universität Mainz (Geographisches Institut, Bodenkunde), Universität Rostock (Professur für Bodenphysik und Ressourcenschutz, Professur für Landschaftsökologie und Standortkunde, Professur für Hydrologie), Kees Vegelin, ZALF (Institut für Bodenlandschaftsforschung, Institut für Landschaftsbiogeochemie), Werner Kutsch, Christian Brümmer, und Miriam Hurkuck. Furthermore, we acknowledge Maik Hunziger and Sören Gebbert for field and GRASS support, Katharina Leiber-Sauheitl, Stefan Frank, Ullrich Dettmann and René Dechow for data processing support, and Annette Freibauer for reviewing the paper draft. The study was financially supported by the joint research project “Organic soils” funded by the Thünen Institute.

References

Bartholomeus, R., Witte, J. P. M., van Bodegom, P. M., and Aerts, R.: The need of data harmonization to derive robust empirical relationships between soil conditions and vegetation, J. Veg. Sci., 19, 799–808, doi:10.3170/2008-8-18450, 2008.

Berglund, O. and Berglund, K.: Influence of water table level and soil properties on emissions of greenhouse gases from cultivated peat soil, Soil Biol. Biochem., 43, 923–931, doi:10.1016/j.soilbio.2011.01.002, 2011.

Beven, K. J. and Kirby, M.: A physically based variable contributing area model of catchment hydrology, Hydrol. Sci. Bull., 24, 43–69, 1979.

Bierkens, M. F. P. and Stroet, C. B. M. T.: Modelling non-linear water table dynamics and specific discharge through landscape analysis, J. Hydrol., 332, 412–426, doi:10.1016/j.jhydrol.2006.07.011, 2007.

Bierkens, M. F. P., Knotters, M., and van Geer, F. C.: Calibration of transfer function-noise models to sparsely or irregularly observed time series, Water Resour. Res., 35, 1741–1750, doi:10.1029/1999wr900083, 1999.

HESSD
11, 3857–3909, 2014

Buchanan, S. and Triantafilis, J.: Mapping water table depth using geophysical and environmental variables, Groundwater, 47, 80–96, doi:10.1111/j.1745-6584.2008.00490.x, 2009.
Clapcott, J., Young, R., Goodwin, E., Leathwick, J., and Kelly, D.: Relationships between multiple land-use pressures and individual and combined indicators of stream ecological integrity, Department of Conservation, DOC Research and Development series 326, Wellington, New Zealand, 2011.
De'ath, G.: Boosted trees for ecological modeling and prediction, Ecology, 88, 243–251, doi:10.1890/0012-9658(2007)88[243:Btfema]2.0.Co;2, 2007.
Dormann, C. F., Elith, J., Bacher, S., Buchmann, C., Carl, G., Carre, G., Marquez, J. R. G., Gruber, B., Lafourcade, B., Leitao, P. J., Munkemuller, T., McClean, C., Osborne, P. E., Reineking, B., Schroder, B., Skidmore, A. K., Zurell, D., and Lautenbach, S.: Collinearity: a review of methods to deal with it and a simulation study evaluating their performance, Ecography, 36, 27–46, doi:10.1111/j.1600-0587.2012.07348.x, 2013.
Drösler, M., Freibauer, A., Adelmann, W., Augustin, J., Bergmann, L., Beyer, C., Chojnicki, B., Förster, C., Giebels, M., Görlitz, S., Höper, H., Kantelhardt, J., Liebersbach, H., Hahn-Schöfl, M., Minke, M., Petschow, U., Pfadenhauer, J., Schaller, L., Schägner, P., Sommer, M., Thuille, A., and Wehrhan, M.: Klimaschutz durch Moorschutz in der Praxis, Ergebnisse aus dem BMBF-Verbundprojekt "Klimaschutz – Moornutzungsstrategien" 2006–2010, vTI-Arbeitsberichte 4/2011, Braunschweig, Germany, http://literatur.vti.bund.de/digbib_extern/bitv/dn049337.pdf (last access: April 2014), 2011.
Elith, J., Leathwick, J. R., and Hastie, T.: A working guide to boosted regression trees, J. Anim. Ecol., 77, 802–813, doi:10.1111/j.1365-2656.2008.01390.x, 2008.
Fan, Y. and Miguez-Macho, G.: A simple hydrologic framework for simulating wetlands in climate and earth system models, Clim. Dynam., 37, 253–278, doi:10.1007/s00382-010-0829-8, 2011.
Fell, H., Roßkopf, N., and Zeitz, J.: Organic soils in Germany, their distribution and carbon stocks, Catena, in preparation, 2014.
Finke, P. A., Brus, D. J., Bierkens, M. F. P., Hoogland, T., Knotters, M., and de Vries, F.: Mapping groundwater dynamics using multiple sources of exhaustive high resolution data, Geoderma, 123, 23–39, doi:10.1016/j.geoderma.2004.01.025, 2004.
Gong, J. N., Wang, K. Y., Kellomaki, S., Zhang, C., Martikainen, P. J., and Shurpali, N.: Modeling water table changes in boreal peatlands of Finland under changing climate conditions, Ecol. Model., 244, 65–78, doi:10.1016/j.ecolmodel.2012.06.031, 2012.

HESSD
11, 3857–3909, 2014

Hahn-Schöfl, M., Zak, D., Minke, M., Gelbrecht, J., Augustin, J., and Freibauer, A.: Organic sediment formed during inundation of a degraded fen grassland emits large fluxes of CH_4 and CO_2, Biogeosciences, 8, 1539–1550, doi:10.5194/bg-8-1539-2011, 2011.

Hijmans, R. J.: Species distribution modeling. Documentation on the R Package "dismo", version 0.9-3, available at: http://cran.r-project.org/web/packages/dismo/dismo.pdf, (last access: February 2014), 2013.

Hoogland, T., Heuvelink, G. B. M., and Knotters, M.: Mapping water-table depths over time to assess desiccation of groundwater-dependent ecosystems in the Netherlands, Wetlands, 30, 137–147, doi:10.1007/s13157-009-0011-4, 2010.

IPCC: IPCC guidelines for national greenhouse gas inventories, edited by: Eggleston, H. S., Buendia, L., Miwa, K., and Ngara, T. K. T., IGES, Japan, 2006.

Ju, W. M., Chen, J. M., Black, T. A., Barr, A. G., Mccaughey, H., and Roulet, N. T.: Hydrological effects on carbon cycles of Canada's forests and wetlands, Tellus B, 58, 16–30, doi:10.1111/j.1600-0889.2005.00168.x, 2006.

Knotters, M. and van Walsum, P. E. V.: Estimating fluctuation quantities from time series of water-table depths using models with a stochastic component, J. Hydrol., 197, 25–46, doi:10.1016/S0022-1694(96)03278-7, 1997.

Leathwick, J. R., Elith, J., Francis, M. P., Hastie, T., and Taylor, P.: Variation in demersal fish species richness in the oceans surrounding New Zealand: an analysis using boosted regression trees, Mar. Ecol.-Prog. Ser., 321, 267–281, doi:10.3354/Meps321267, 2006.

Leiber-Sauheitl, K., Fuß, R., Voigt, C., and Freibauer, A.: High CO_2 fluxes from grassland on histic Gleysol along soil carbon and drainage gradients, Biogeosciences, 11, 749–761, doi:10.5194/bg-11-749-2014, 2014.

Levy, P. E., Burden, A., Cooper, M. D. A., Dinsmore, K. J., Drewer, J., Evans, C., Fowler, D., Gaiawyn, J., Gray, A., Jones, S. K., Jones, T., Mcnamara, N. P., Mills, R., Ostle, N., Sheppard, L. J., Skiba, U., Sowerby, A., Ward, S. E., and Zielinski, P.: Methane emissions from soils: synthesis and analysis of a large UK data set, Global Change Biol., 18, 1657–1669, doi:10.1111/j.1365-2486.2011.02616.x, 2012.

Limpens, J., Berendse, F., Blodau, C., Canadell, J. G., Freeman, C., Holden, J., Roulet, N., Rydin, H., and Schaepman-Strub, G.: Peatlands and the carbon cycle: from local processes to global implications – a synthesis, Biogeosciences, 5, 1475–1491, doi:10.5194/bg-5-1475-2008, 2008.

HESSD
11, 3857–3909, 2014

Martin, M. P., Wattenbach, M., Smith, P., Meersmans, J., Jolivet, C., Boulonne, L., and Arrouays, D.: Spatial distribution of soil organic carbon stocks in France, Biogeosciences, 8, 1053–1065, doi:10.5194/bg-8-1053-2011, 2011.

Melton, J. R., Wania, R., Hodson, E. L., Poulter, B., Ringeval, B., Spahni, R., Bohn, T., Avis, C. A., Beerling, D. J., Chen, G., Eliseev, A. V., Denisov, S. N., Hopcroft, P. O., Lettenmaier, D. P., Riley, W. J., Singarayer, J. S., Subin, Z. M., Tian, H., Zürcher, S., Brovkin, V., van Bodegom, P. M., Kleinen, T., Yu, Z. C., and Kaplan, J. O.: Present state of global wetland extent and wetland methane modelling: conclusions from a model inter-comparison project (WETCHIMP), Biogeosciences, 10, 753–788, doi:10.5194/bg-10-753-2013, 2013.

Moore, T. R. and Dalva, M.: The influence of temperature and water-table position on carbon-dioxide and methane emissions from laboratory columns of peatland soils, J. Soil Sci., 44, 651–664, doi:10.1111/j.1365-2389.1993.tb02330.x, 1993.

Moore, T. R. and Roulet, N. T.: Methane flux – water-table relations in northern wetlands, Geophys. Res. Lett., 20, 587–590, doi:10.1029/93gl00208, 1993.

Nash, J. E. and Sutcliffe, J. V.: River flow forecasting through conceptual models part I – A discussion of principles, J. Hydrol., 10, 282–290, doi:10.1016/0022-1694(70)90255-6, 1970.

Regina, K., Nykänen, H., Silvola, J., and Martikainen, P. J.: Fluxes of nitrous oxide from boreal peatlands as affected by peatland type, water table level and nitrification capacity, Biogeochemistry, 35, 401–418, doi:10.1007/BF02183033, 1996.

Ridgeway, G.: Generalized boosted regression models, Documentation on the R Package "gbm", version 2.1, available at: http://cran.r-project.org/web/packages/gbm/gbm.pdf (last access: February 2014), 2013.

Sutanudjaja, E. H., van Beek, L. P. H., de Jong, S. M., van Geer, F. C., and Bierkens, M. F. P.: Using ERS spaceborne microwave soil moisture observations to predict groundwater head in space and time, Remote Sens. Environ., 138, 172–188, doi:10.1016/j.rse.2013.07.022, 2013.

Tetzlaff, B., Kuhr, P., and Wendland, F.: A new method for creating maps of artificially drained areas in large river basins based on aerial photographs and geodata, Irrig. Drain., 58, 569–585, doi:10.1002/Ird.426, 2009.

Thompson, J. R., Gavin, H., Refsgaard, A., Sorenson, H. R., and Gowing, D. J.: Modelling the hydrological impacts of climate change on UK lowland wet grassland, Wetl. Ecol. Manage., 17, 503–523, doi:10.1007/s11273-008-9127-1, 2009.

HESSD
11, 3857–3909, 2014

UBA: National Inventory Report for the German Greenhouse Gas Inventory 1990–2008, Submission under the United Nations Framework Convention on Climate Change and the Kyoto Protocol 2012, Dessau, Germany, 2012.

van der Gaast, J. W. J., Massop, H. T. L., and Vroon, H. R. J.: Actuele grondwaterstandsituatie in natuurgebieden: Een. Pilotstudie, Wettelijke Onderzoekstaken Natuur & Milieu, WOt-rapport 94, Wageningen, 2009.

van der Ploeg, M. J., Appels, W. M., Cirkel, D. G., Oosterwoud, M. R., Witte, J. P. M., and van der Zee, S. E. A. T. M.: Microtopography as a driving mechanism for ecohydrological processes in shallow groundwater systems, Vadose Zone J., 11, 52–62, doi:10.2136/vzj2011.0098, 2012.

HESSD

11, 3857–3909, 2014

Table 1. Overview on predictor variables.

Predictor Variable	Variable name	Values	Point/Buffers (m)	Data Source
Land use type		Arable, grassland, forest, shrubs, peat-mining, unused peatland, swamp, open water	point, 100, 500, 1000, 2500	Digital Landscape Model[1]
Vegetation attributes (optional)		Deciduous forest, mixed forest, coniferous forest, reed, shrubs, grass	point	Digital Landscape Model[1]
"Wet soil observed"		Yes, no	point	Digital Landscape Model[1]
Combined land cover information (land use type + veg. + wet soil attr.)	lc	Arable, grassland, wet grassland, deciduous including mixed forest, wet forest, coniferous forest, reed, unused peatland, wet unused peatland	point, 100, 500, 1000, 2500	Digital Landscape Model[1]
Dry land cover fraction	$f_{dry}(X)$	arable + 0.5 · grassland on organic soil area; 0 to 1	100, 500, 1000, 2500	Digital Landscape Model[1]
Wet land cover fraction		reed + wet grassland + wet forest + wet unused peatland on organic soil area; 0 to 1	100, 500, 1000, 2500	Digital Landscape Model[1]
Total length of ditches for all lc and only for arable and grassland (subscr.: "*dry*")	$di_{len,\,dry}(X)$	≥ 0 m	point, 50, 250, 1000, 2500	Digital Landscape Model[1]
Distance to next ditch		≥ 0 m	point	Digital Landscape Model[1]
Peatland type	p_{type}	Lowland bog, upland bog, fen neighboring surface water, fen without neighboring surface water, other "low-C" organic soil	point	Map of organic soils[2]
Material at peat base	p_{base}	Unconsolidated rock, peat clay layer, rock, no information	point	Map of organic soils[2]
Peatland fraction	$f_{peat}(X)$	0 to 1	point, 500, 1000, 2500	Geological Map (BGR)[3]
Distance to edge of peatland		> 0 m		Geological Map (BGR)[3]
Ratio of d_{peat}/f_{peat}		> 0	2500	Geological Map (BGR)[3]
Precipitation		≥ 0 mm	point	raster map 1 km × 1 km (DWD)[4]
Evapotranspiration		≥ 0 mm	point	raster map 1 km × 1 km (DWD)[4]
Climatic water balance	wb_{summer}	< 0 and ≥ 0 mm	point	raster map 1 km × 1 km (DWD)[4]
Relative height	$h_{rel}(X)$	< 0 and ≥ 0 m	point – median 25, 50, 100, 250, 500, 1000	Digital Elevation Model[5]
Topographic index	$ti_{rasR}(X)$	> 0	point and 1000 buffer for 10, 25, 250, 1000 raster values	Digital Elevation Model[5]
Protection status		Nature Conservation Area, Special Areas of Conservation, Special Protection Area for wild birds, UNESCO-biosphere reserve, Nature Park, National Park, Landscape Protection Area	point	Maps of protected areas[6]

[1] ATKIS Basis DLM, Federal Agency for Cartography and Geodesy, BKG;
[2] Map of organic soils (Fell et al., 2014, Humboldt University of Berlin);
[3] Geological Map 1 : 200 000 (GUEK 200, BGR – Federal Institute for Geosciences and Natural Resources);
[4] raster map 1 km × 1 km of weather data (German Weather Service);
[5] BKG; Variable name indicated for the nine variables in the final model with (X) indicating buf. size and R indicating raster resolution.
[6] Federal Agency for Nature Conservation (BfN).

HESSD
11, 3857–3909, 2014

Table 2. Weighted mean and standard deviation of WL and WL_t data, and of the WL_t map presented in Sect. 3.6, for the nine land cover classes.

	WL (m) mean ± sd	WL_t (–) mean ± sd	WL_t (–), map mean ± sd
arable land	−0.69 ± 0.30	−0.76 ± 0.17	−0.66 ± 0.22
deciduous f.	−0.45 ± 0.34	−0.49 ± 0.37	−0.47 ± 0.35
grassland	−0.44 ± 0.29	−0.52 ± 0.32	−0.49 ± 0.30
unused peatl.	−0.39 ± 0.36	−0.39 ± 0.41	−0.37 ± 0.40
coniferous f.	−0.36 ± 0.36	−0.37 ± 0.37	−0.46 ± 0.35
wet unused peatl.	−0.22 ± 0.27	−0.18 ± 0.40	−0.17 ± 0.36
wet forest	−0.22 ± 0.29	−0.17 ± 0.43	−0.21 ± 0.39
wet grassland	−0.10 ± 0.14	−0.00 ± 0.31	−0.15 ± 0.39
reed	−0.01 ± 0.17	0.20 ± 0.29	−0.06 ± 0.32

HESSD
11, 3857–3909, 2014

Table 3. Performance criteria of the different models; dry range defined as WL < −0.3 m and wet range as WL > −0.3 m.

	WL (m) (calibrated on WL)	WL_t (–) (calibrated on WL)	WL_t (–) (calibrated on WL_t)
NSE_{cal}	0.627	0.559	0.642
NSE_{cv}	0.381	0.397	0.453
$RMSE_{cv}$	0.269	0.299	0.284
$RMSE_{cv,\ dry}$	0.284	0.263	0.259
$RMSE_{cv,\ wet}$	0.222	0.382	0.355
Bias	−0.003	0.083	0.002
$Bias_{dry}$	−0.012	0.070	0.003
$Bias_{wet}$	0.021	0.120	0.000

HESSD
11, 3857–3909, 2014

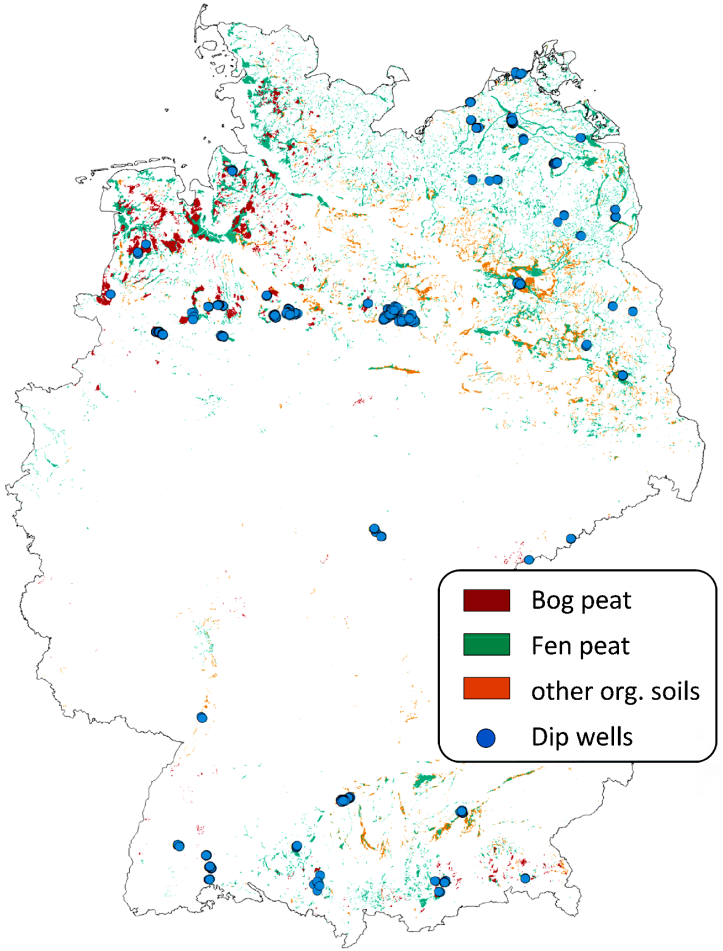

Fig. 1. Locations of the 1094 dip wells of the dataset. Base map (Geological map 1 : 200 000, BGR) shows the distribution of bog and fen peat, and other organic soils.

HESSD
11, 3857–3909, 2014

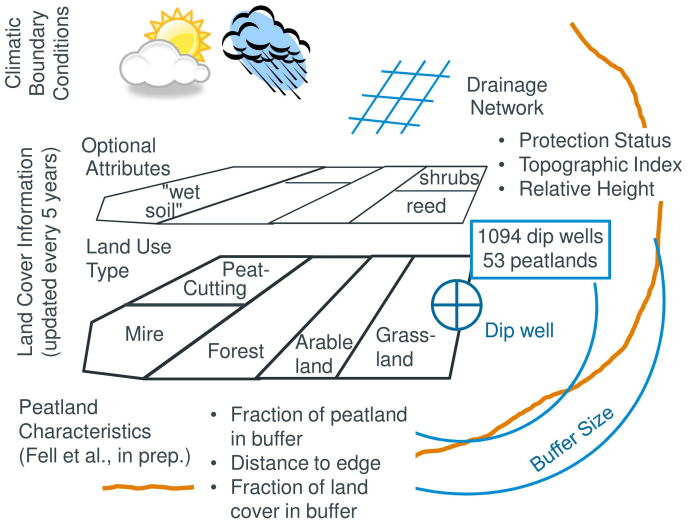

Fig. 2. Illustration of the predictor variables determined for each dip well based on available national maps (see Table 1).

HESSD
11, 3857–3909, 2014

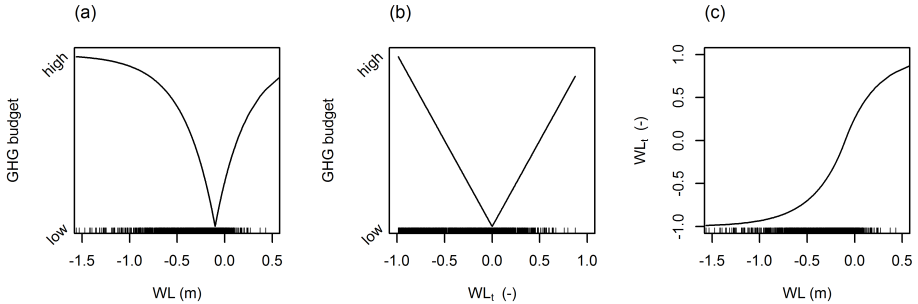

Fig. 3. Illustration of the annual mean water level (WL) transformation. **(a)** Hypothetical transfer function relating GHG budget to WL (m). **(b)** GHG budget vs. the transformed water level (WL_t). **(c)** WL_t vs. WL. Rugs indicate the data quantiles of the analyzed dataset.

HESSD
11, 3857–3909, 2014

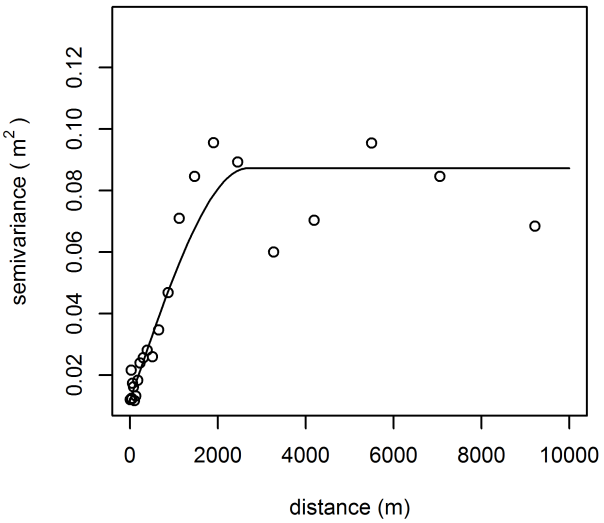

Fig. 4. Sample semi-variogram and fitted semi-variogram model of the annual mean water level data, WL.

HESSD
11, 3857–3909, 2014

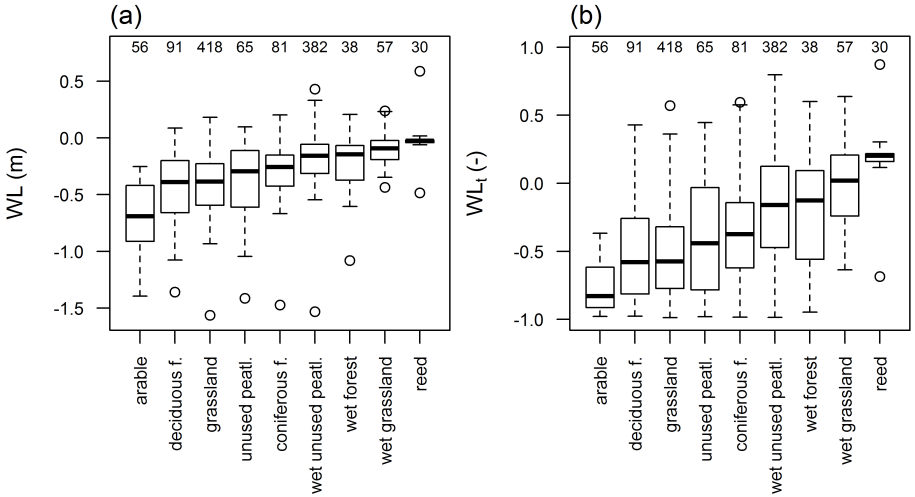

Fig. 5. Water level relative to ground surface, WL (m), and transformed water level, WL_t (–), by land cover class illustrated as weighted box plot. $WL_t = -1$ corresponds to maximum CO_2 emissions and $WL_t = 1$ to maximum CH_4 emissions. In the upper part, the number of dip wells in each class is indicated.

HESSD
11, 3857–3909, 2014

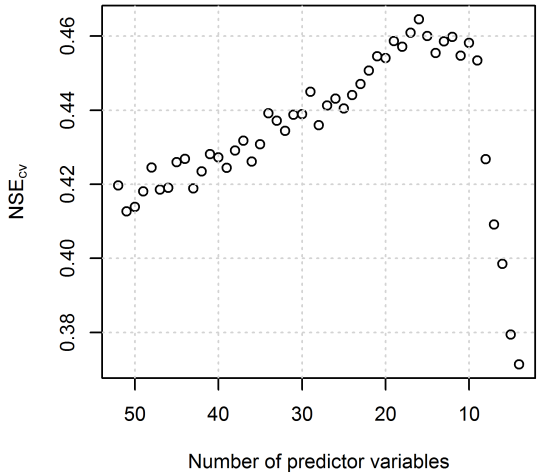

Fig. 6. NSE$_{cv}$ as a function of number of predictor variables used in the model of WL$_t$ during model simplification and shown for the last 50 parameter drops.

HESSD
11, 3857–3909, 2014

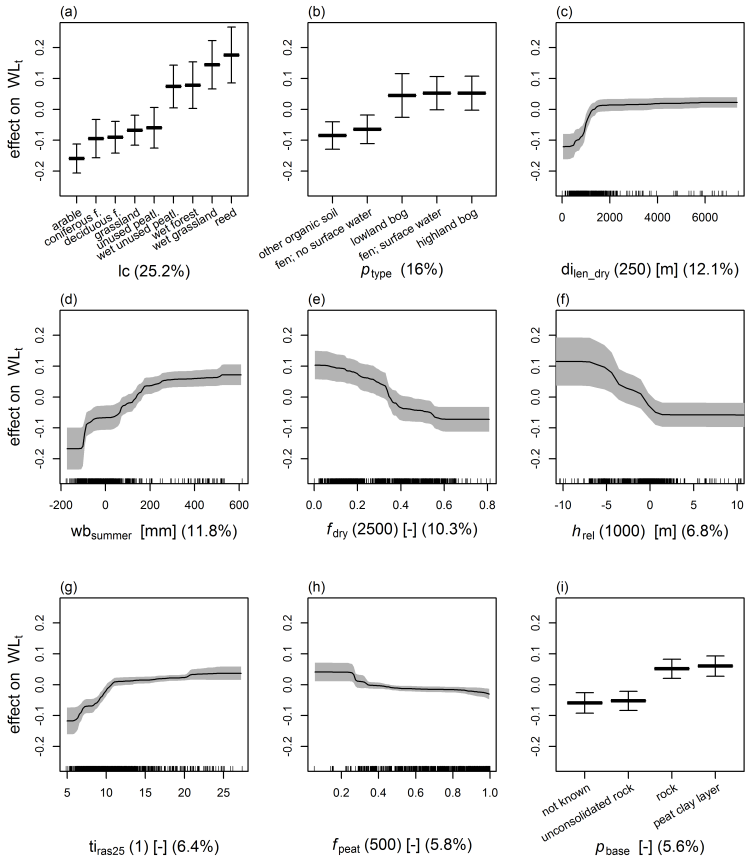

Fig. 7. Partial dependence plots for the predictor variables. For explanation of variables see Table 1. *Y* axes are on WL_t scale and are centered around the mean WL_t. Error bars and grey area indicate standard deviation of the response over 1000 bootstrap models. The relative contribution of each predictor is indicated as percentage. Rugs at bottom of each plot show distribution of data across that variable, in deciles.

HESSD
11, 3857–3909, 2014

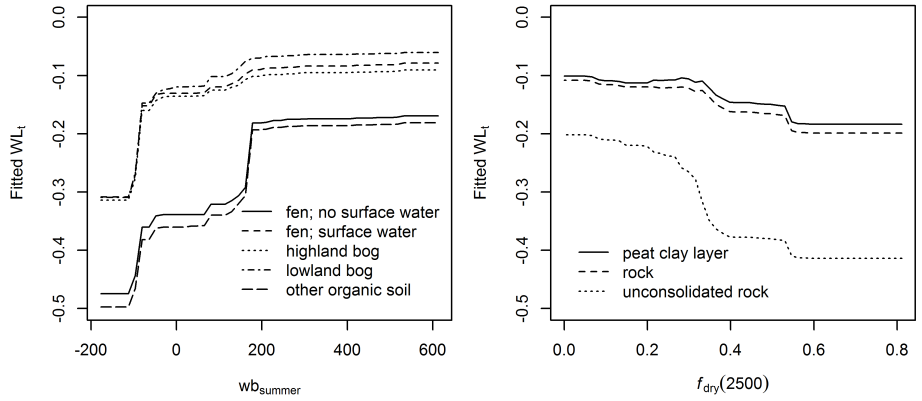

Fig. 8. Partial dependence plots representing the two strongest interactions in the model: **(a)** between p_{type} and wb_{summer} and **(b)** between p_{base} and f_{dry}. Fitted WL_t is plotted on the y-axis which is obtained after accounting for the average effect of all other predictor variables.

HESSD
11, 3857–3909, 2014

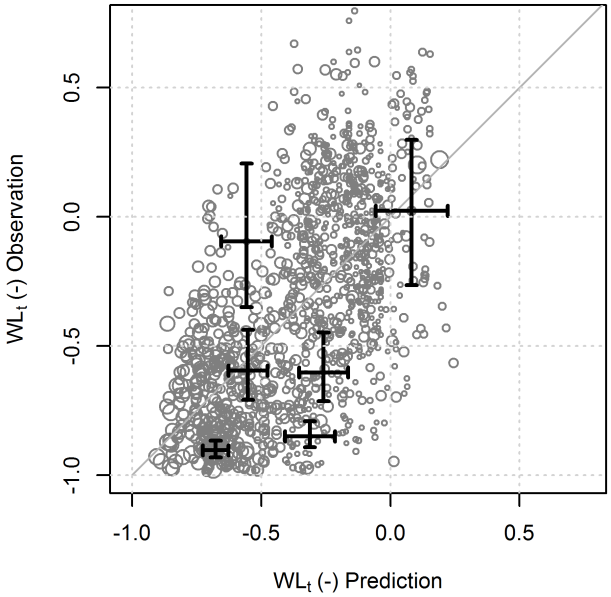

Fig. 9. Observed vs. predicted transformed annual mean water level (WL_t) from cross-validation results. Error bars show selected data and bootstrap model errors as standard deviation. Data points are scaled by their weights.

HESSD
11, 3857–3909, 2014

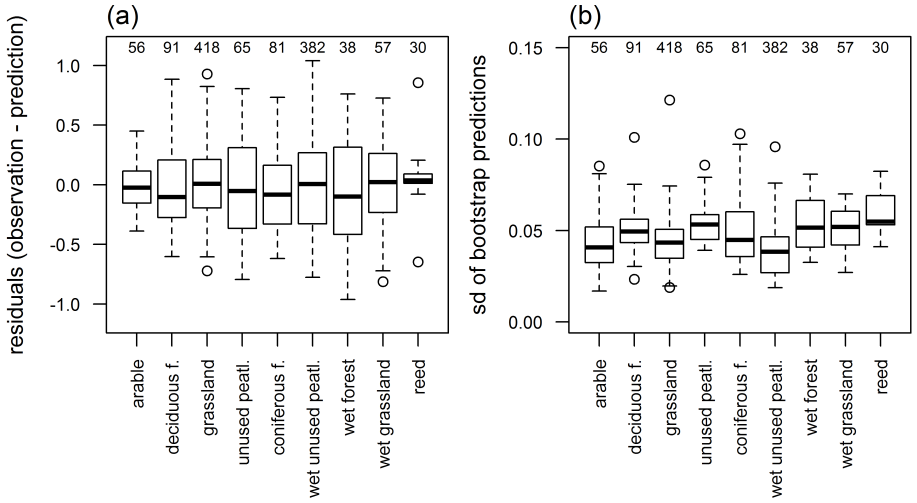

Fig. 10. (a) Residuals (observation – prediction) of WL_t predictions and **(b)** standard deviation (sd) of bootstrap predictions shown for the nine land cover classes. In the upper part, the number of dip wells in each class is indicated.

HESSD
11, 3857–3909, 2014

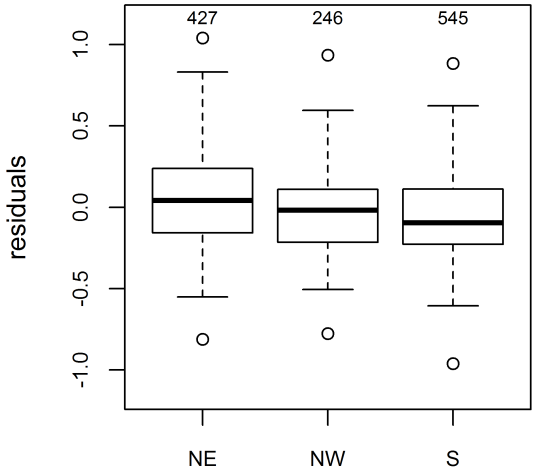

Fig. 11. Residuals (observation – prediction) of WL_t predictions for the three major geographical peatland regions of Germany. In the upper part, the number of dip wells in each class is indicated.

HESSD
11, 3857–3909, 2014

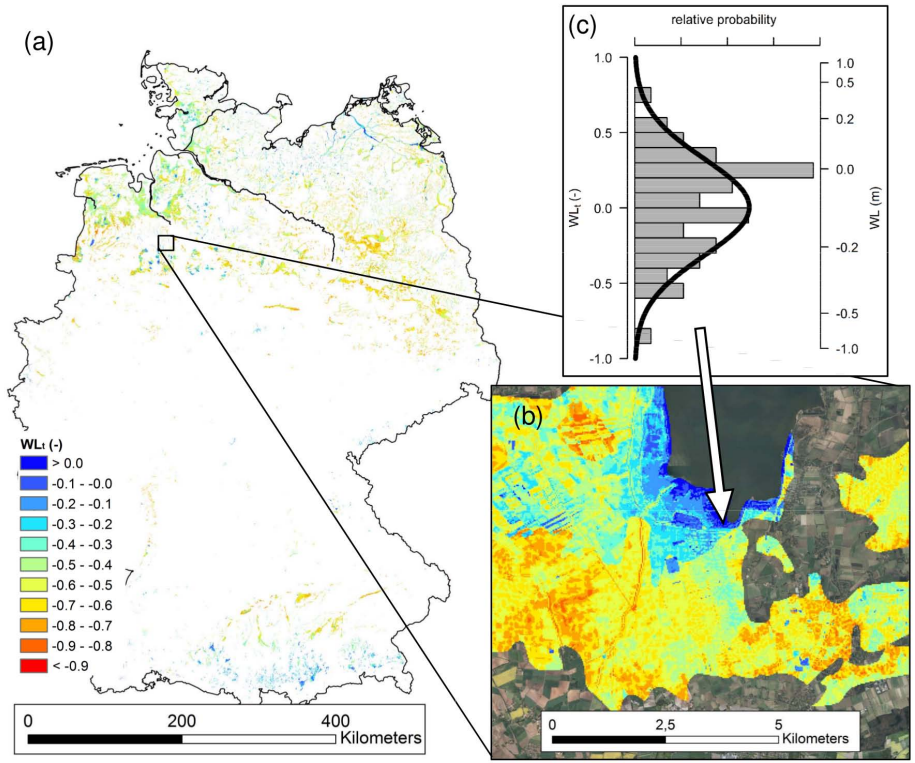

Fig. 12. Map of predictions of transformed annual mean water level (WL_t) for all German organic soils **(a)** and an enlarged map section **(b)**. Probability distribution in **(c)** exemplarily indicates the uncertainty of a specific point prediction for wet grassland. Here, predicted value is approximately $WL_t = 0$, but note that wet grassland predictions do vary in space depending on the values of the other model parameter. The histogram shows the residuals from cross-validation for wet grassland, to which the probability distribution was fitted.

HESSD
11, 3857–3909, 2014

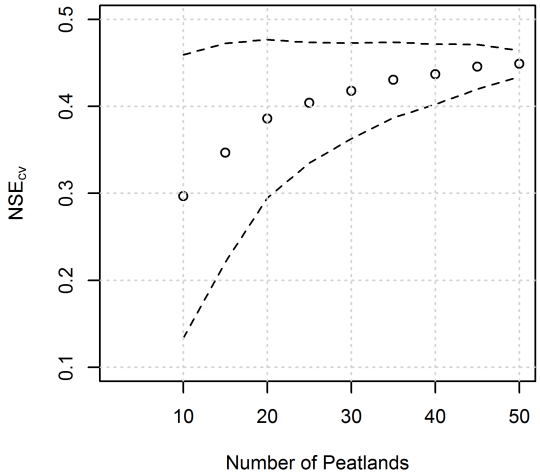

Fig. 13. NSE of cross-validation vs. number of randomly selected peatland areas. Dashed lines indicate $NSE_{cv} \pm$ standard deviation.

HESSD
11, 3857–3909, 2014